Separation Science and Technology
Publication details, including instructions for authors and subscription information:
http://www.informaworld.com/smpp/title~content=t713708471

Effect of Si/Al Ratio on CO_2 - CH_4 Adsorption and Selectivity in Synthesized SAPO-34

S. Siamak Ashraf Talesh[a]; S. Fatemi[a]; S. J. Hashemi[a]; M. Ghasemi[b]
[a] Chemical Engineering Department, Faculty of Engineering, University of Tehran, Tehran, Iran [b] Petroleum Industrial Institute, Tehran, Iran

To cite this Article Talesh, S. Siamak Ashraf , Fatemi, S. , Hashemi, S. J. and Ghasemi, M.(2010) 'Effect of Si/Al Ratio on CO_2 - CH_4 Adsorption and Selectivity in Synthesized SAPO-34', Separation Science and Technology, 45: 9, 1295 — 1301
To link to this Article: DOI: 10.1080/01496391003684414
URL: http://dx.doi.org/10.1080/01496391003684414

Separation Science and Technology, 45: 1295–1301, 2010
Copyright © Taylor & Francis Group, LLC
ISSN: 0149-6395 print/1520-5754 online
DOI: 10.1080/01496391003684414

Effect of Si/Al Ratio on CO_2 – CH_4 Adsorption and Selectivity in Synthesized SAPO-34

S. Siamak Ashraf Talesh,[1] S. Fatemi,[1] S. J. Hashemi,[1] and M. Ghasemi[2]
[1]*Chemical Engineering Department, Faculty of Engineering, University of Tehran, Tehran, Iran*
[2]*Petroleum Industrial Institute, Tehran, Iran*

Impact of Si/Al ratio on the adsorption capacity and separation selectivity of CO_2/CH_4 in SAPO-34 has been investigated. SAPO-34 samples were synthesized with two Si/Al ratios (0.2 and 0.3). A batch adsorption volumetric apparatus was used to measure the adsorption equilibrium capacity and derive the equilibrium isotherms. The tests were performed in a wide range of pressure from normal to 3000 kPa and three levels of temperatures from 277 to 298 K. Results proved decreasing Si/Al ratio, from 0.3 to 0.2, improved CO_2 separation from CH_4.

Keywords adsorption; CO_2/CH_4 separation; molecular sieve; SAPO-34; Si/Al ratio; silicoaluminophosphate; synthesis

INTRODUCTION

Elimination and separation of CO_2 from gas mixtures such as natural gas, industrial biogas by-products and land fill gas have received great attention in recent research (1). CO_2 with its acidic property causes corrosion in storage tanks and pipelines. It also reduces the energy content of natural gas. Furthermore, natural gas containing a significant amount of CO_2 needs to be upgraded to meet the pipeline regulations to prevent gas condensation. The preferred methods for separation of CO_2 from gas mixtures include absorption, cryogenic, adsorption, and membrane technology. Traditional process of removing CO_2 is amine washing (absorption), which is a toxic and environmentally hostile technique (2). Separation of gas mixtures by adsorption is an economic and efficient process especially using new synthesized molecular sieves, which has been improved in recent years.

Adsorbent selection is the main step to achieve an effective adsorption process. The kinetic diameter of the gas component, adsorbent pore diameter, and surface properties are the physical key parameters in diffusion of the adsorbate molecules from the pore mouths into the porous structure of the adsorbents. Microporous materials with pore size near molecular dimensions, such as zeolites, aluminophosphate (ALPO), and silicoaluminophosphate (SAPO) molecular sieves are recently introduced to membrane technology (3). SAPO-34 as a novel molecular sieve among the SAPOs family with CHA structure, has been attracting much more attention in separation applications due to its three-dimensional cages, small pore diameter, and moderate acidic surface property (4). This material with a pore diameter of 0.38 nm has been selected after many investigations among the various types of SAPOs as the best candidate for the selective separation of CO_2 (0.33 nm kinetic diameter) from CH_4 (0.38 nm diameter) (4,5). In contrast, the other forms of SAPOs such as SAPO-5, SAPO-41, SAPO-11, SAPO-18 and SAPO-44 have a one-dimensional structure and/or with a pore size larger than 0.38 nm would let both CO_2 and CH_4 diffuse through the pores (5).

In preparation, process factors such as chemical composition, source of components, template type, aging, crystallization time, and temperature affect the synthesized phase (6–10). Si/Al ratio plays an important role in the adsorption of CO_2 against CH_4 in zeolite or zeotype molecular sieves. By increasing the Si/Al ratio cationic density of zeolite enhances, which promotes the adsorption of polar or quadrupolar molecules such as CO_2. Adsorption of CO_2 and CH_4 has been studied using various type of adsorbents and membranes such as X, Y, all-silica DD3R, β-Zeolite, ZSM-5, SAPO-34 (11–17).

This work is an attempt to prepare an appropriate molecular sieve, SAPO-34, in order to improve the selective adsorption of CO_2 versus CH_4 and investigate the effect of Si/Al ratio on the adsorption capacity. Although various stoichiometries have been proposed for synthesis of SAPO-34 in previous works (18,25–27), the stoichiometry applied in this study has not been reported to date. The synthesized samples of SAPO-34 with two Si/Al ratios (0.2 and 0.3) have been tested for the adsorption capacity and selectivity at atmospheric pressure up to 3000 kPa and three temperature levels.

Received 28 March 2009; accepted 26 January 2010.

Address correspondence to S. Fatemi, Chemical Engineering Department, Faculty of Engineering, POB 11365-4563, University of Tehran, Enghlab Avenue, Tehran, Islamic Republic of Iran. Fax: +982166957784. E-mail: shfatemi@ut.ac.ir

It should be noted that previous investigations did not consider pressures beyond atmospheric pressure, however, there are some studies on SAPO-34 at low pressures (1,16–26). To fill this gap, we studied the performance of SAPO-34 at a wide range of pressure above the temperature.

EXPERIMENTAL

Synthesis

SAPO-34 was prepared by in situ crystallization and hydrothermal transformation, with two Si/Al ratios. Fine crystals were synthesized from a sol-gel medium with chemical composition of Al_2O_3:$x$$SiO_2$:$P_2O_5$:1.2 TEAOH: 47 H_2O, where x could be 0.4 or 0.6. The reactants consisted of silica gel 60 (Merck), Aluminium isopropoxide (Merck), and phosphoric acid (85 wt% aqueous solution, Merck). Tetraethyl ammonium hydroxide (TEAOH, 35 wt% aqueous solution, Aldrich) was used as a template agent.

To prepare the colloidal gel, deionized water and phosphoric acid were mixed together, and aluminium isopropoxide was added gradually under high speed stirring for 12 h at 2°C. Thereafter silica gel and TEAOH were added to the solution, respectively. Prior to the crystallization process, the solution was aged under 600 rpm agitation at room temperature for 24 h. The prepared gel was transferred to a Teflon-lined stainless steel autoclave. Hydrothermal synthesis was carried out at 463 K for 24 h. The product was washed thoroughly with deionized water and centrifuged three times. Finally, the product was calcined in a static air furnace at 823 K for 6 h at the heating rate of 1°C/min. The experimental conditions are summarized in Table 1.

Characterization

The calcined powder was characterized by the X-Ray Diffraction (XRD) and Scanning Electron Microscopic (SEM) analysis. The XRD pattern was recorded on a Philips analytical X-ray diffractometer with Cu Kα radiation (wavelength; $\lambda = 1.54$). The crystal morphology was analyzed by Scanning Electron Microscopy.

Adsorption Experiments

The adsorption isotherms were obtained by using a volumetric apparatus at atmospheric and higher pressures up to 3000 kPa for three temperature levels. A schematic diagram of the adsorption set up is shown in Fig. 1. To examine the adsorbents performance, the samples, S_1 and S_2, were loaded into the adsorption cell and pretreated prior to adsorption experiments. The pretreatment was carried out under vacuum and 453 K for 6 h. Then the equilibrium isotherm tests for CO_2 and CH_4 were conducted at three temperatures (278, 288, and 298 K) and operating gauge pressures varying from 100 to 3000 kPa (100, 500, 1000, 1500, 2000, 2500, 3000 kPa). The amount of the adsorbed material was determined by measuring the system pressure before and after equilibrium by means of a pressure sensor with 0.1% full scale precision. The detailed procedure has been explained elsewhere (28).

RESULTS AND DISCUSSION

Product Characterization

Figure 2 shows the XRD pattern for the two synthesized samples. The XRD patterns of S_1 and S_2 SAPO-34 samples were essentially similar (Fig. 2) and well matched with that of SAPO-34 reported by Prakash (29).

SEM images (Fig. 3), proved presence of cubic SAPO-34 crystals smaller than 2 µm. There was no significant difference in the average size and size distribution of the samples.

Adsorption Isotherms

Methane and carbon dioxide isotherms were well described by the Toth model employing the following formula (30):

$$\theta = \frac{q_i}{q^{sat}} = \frac{(bp)^{1/n}}{(1 + (bp)^n)^{1/n}} \tag{1}$$

The parameters of the Toth model for each temperature are listed in Table 2. For the pressure range studied here, the correlation coefficient was 0.999 at any temperature, which showed a good agreement with experimental data.

Figures 4 to 7 demonstrate the adsorption isotherms for CO_2 and CH_4 on the samples. It is evident that the adsorption capacity of CO_2 is higher than that of CH_4 on both adsorbents. The difference between the kinetic diameters of adsorbate molecules, polarizability of CO_2 versus CH_4, high quadrupole moment of CO_2, and heterogeneity of

TABLE 1
Synthesis conditions

Samples	Si/Al	Crystallization time (h)	Crystallization temperature (K)	Calcination temperature (K)	Calcination time (h)
S_1	0.2	24	463	823	6
S_2	0.3				

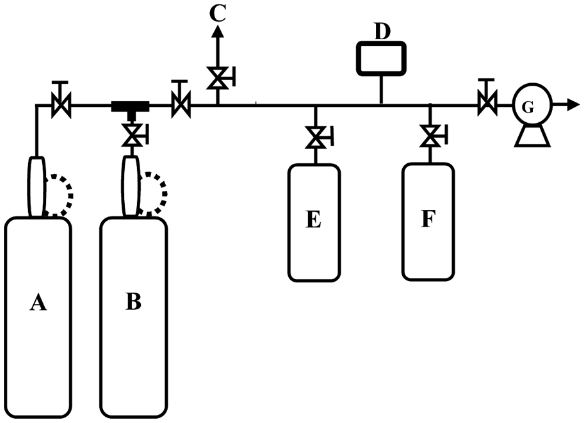

FIG. 1. Schematic of experimental apparatus: A: (CO_2 or CH_4) Cylinder; B: Helium Cylinder; C: vent; D: Pressure transducer (0–4000 kPa); E: Reference gas vessel; F: Adsorption cell; G: Vacuum pump.

the surface (15) may contribute to the higher adsorption capacity.

SAPO-34 is a molecular sieve with 0.38 × 0.38 nm pore diameter. The kinetic diameter of CO_2 and CH_4 are 0.33 nm and 0.38 nm respectively. Therefore CO_2 could pass through the pore mouths of crystals whereas it might be difficult for CH_4, especially at lower pressures. On the other hand, CO_2 has a strong quadrupole moment and a higher tendency to the cationic surface of SAPO-34. In contrast, the nonpolar CH_4 molecules show weak attraction forces with the adsorbent surface that leads to low adsorption capacity. A comparison among Figs. 4 and 6 with Figs. 5 and 7 suggests a larger slope for CO_2 isotherm especially at lower pressures. The results confirm stronger attraction forces between CO_2 and both S_1 and S_2 samples.

Increasing pressure over 1000 kPa showed no significant effect on CO_2 adsorption capacity, while CH4 adsorption continued to increase. As demonstrated in Figs. 4 and 6, S_1(Si/Al = 0.2) adsorbent shows a better performance for CO_2 adsorption compared to S_2 (Si/Al = 0.3). By decreasing the ratio of Si to Al, the surface cationic density and the heterogeneity are enhanced (11). Higher CO_2 adsorption in S_1 is attributed to the higher surface cationic density and more surface heterogeneity.

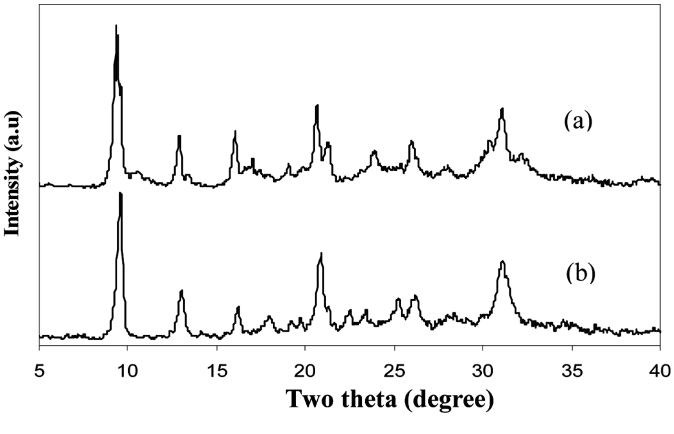

FIG. 2. XRD pattern of samples, (a) S_1; (b) S_2.

Calculated parameters using the Toth model are presented in Table 2. The values confirm the experimental results. System heterogeneity is exhibited by the parameter *n* determined in the Toth isotherm. It is evident that the amount of CO_2 saturation adsorption capacity (q^{sat}) is significantly more than that of CH_4 for both adsorbents. Additionally, CO_2 shows a higher q^{sat} on S_1 compared to S_2. Parameter *n* could be considered as the heterogeneity parameter, lower *n* indicates more surface heterogeneity and higher adsorption capacity for sample S_1.

Heat of Adsorption

Heat of adsorption and its variation with coverage can provide useful information about surface characteristics and the adsorbed phase. The heat of adsorption, ΔH_{ads}, was calculated using the experimental data and Vant Hoff equation:

$$(-\Delta H_{ads})_i = RT^2\left(\frac{\partial \ln P}{\partial T}\right)_{q_i} \tag{2}$$

In Figs. 8 and 9, the heats of adsorption are demonstrated for the two samples as a function of adsorption capacity. As shown in Fig. 8, the heat of adsorption of methane is lower, and exhibits no significant variation with the adsorption amount. This result indicates less active energetic sites for CH_4 adsorption. The heat of adsorption of methane increases slightly with adsorption loading, suggesting that the adsorbate–adsorbate interactions are more pronounced at a higher pressure range (16). On the other hand, the heat of adsorption of CO_2 decreases slightly with increased loading. This reduction implies that the stronger adsorption sites are firstly occupied then followed by weaker sites. The decrease is more significant for sample S_1, which proves the presence of more energetic adsorption sites on that sample.

The average heat of adsorption in the range of adsorption capacity is calculated as follow:

$$(-\Delta H_{ads})_{av} = \frac{\sum q_i \cdot (-\Delta H_{ads})_i}{\sum q_i} \tag{3}$$

The amount of $(\Delta H_{ads})_{av}$ is presented in Table 3.

According to the heat of adsorption values in Table 3, the difference in the heat of adsorption of two gases is higher for S_1. This result could be, once more, contributed to the lower Si/Al ratio that induces more surface heterogeneity, and higher cationic density, which in turn

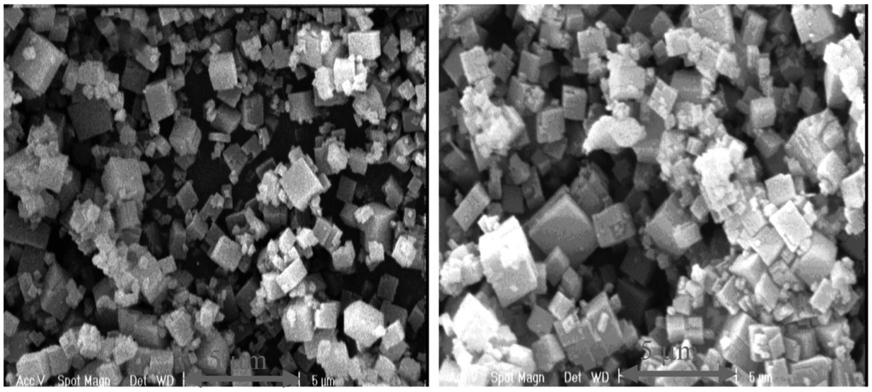

(a) (b)

FIG. 3. SEM photographs of the samples surfaces; (a) S_1, (b) S_2.

enhances the adsorption of polar and quadrupolar molecules such as CO_2.

Adsorption Selectivity

Figures 10 and 11 demonstrate adsorption selectivity of S_1 and S_2 samples for CO_2 and CH_4 at three temperatures as a function of pressure.

The ideal adsorption selectivity was calculated from the ratio of equilibrium adsorption capacity for single gases

TABLE 2
Toth parameters of synthesized SAPO-34

	T = 298 K	T = 288 K	T = 278 K
Sample S_1			
CH_4			
q^{sat} (mmol/g)	2.1897	2.5266	2.7261
$b^{*}100$ $(kPa)^{-1}$	0.0019	0.0022	0.0029
n	1.0489	0.9519	0.8308
R^2	0.999	0.999	0.999
CO_2			
q^{sat} (mmol/g)	4.8093	5.3097	6.8341
$b^{*}100$ $(kPa)^{-1}$	0.0112	0.0202	0.1075
n	0.6567	0.5671	0.3641
R^2	0.999	0.999	0.999
Sample S_2			
CH_4			
q^{sat} (mmol/g)	2.0319	2.3926	2.8073
$b^{*}100$ $(kPa)^{-1}$	0.0014	0.0016	0.0021
n	1.0903	0.9391	0.7614
R^2	0.999	0.999	0.999
CO_2			
q^{sat} (mmol/g)	3.6648	4.0502	4.6270
$b^{*}100$ $(kPa)^{-1}$	0.0079	0.0130	0.0393
n	0.9524	0.8032	0.5613
R^2	0.999	0.999	0.999

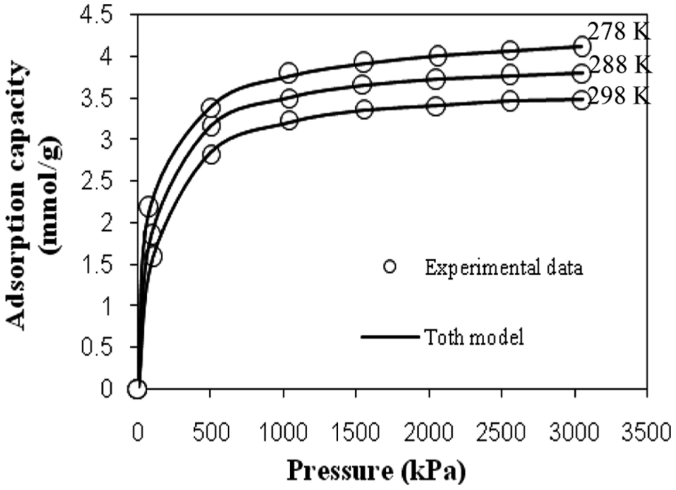

FIG. 4. Adsorption isotherm for CO_2 on S_2 adsorbent.

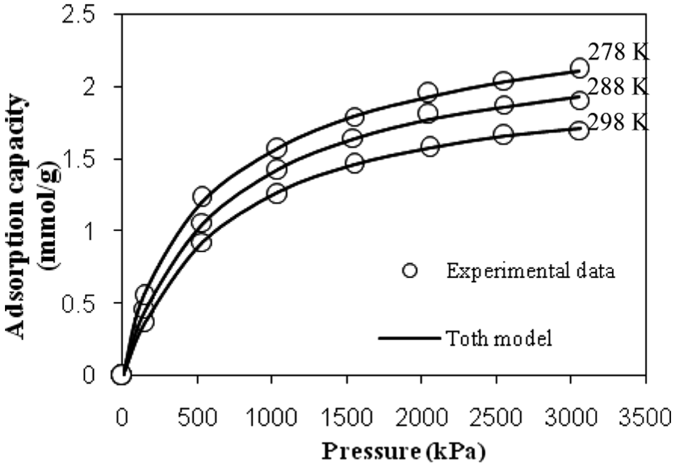

FIG. 5. Adsorption isotherm for CH_4 on S_2 adsorbent.

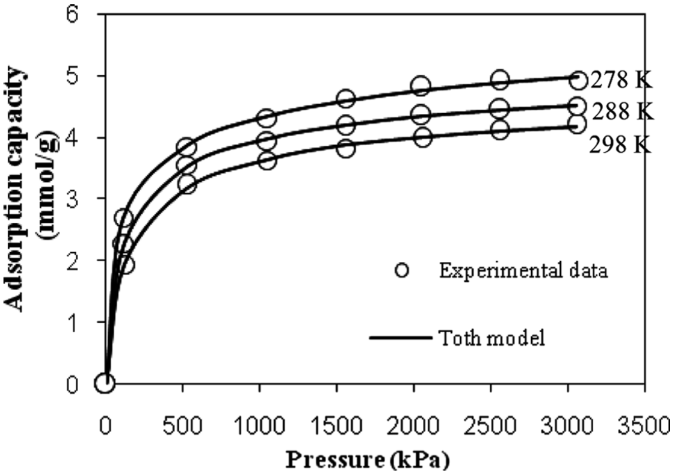

FIG. 6. Adsorption isotherm for CO_2 on S_1 adsorbent.

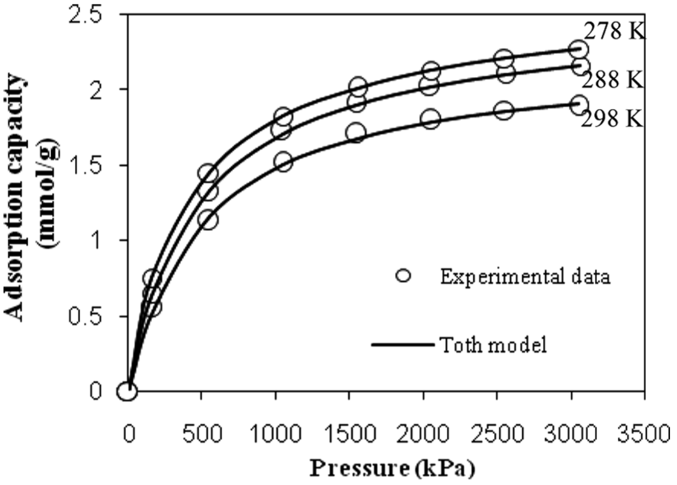

FIG. 7. Adsorption isotherm for CH_4 on S_1 adsorbent.

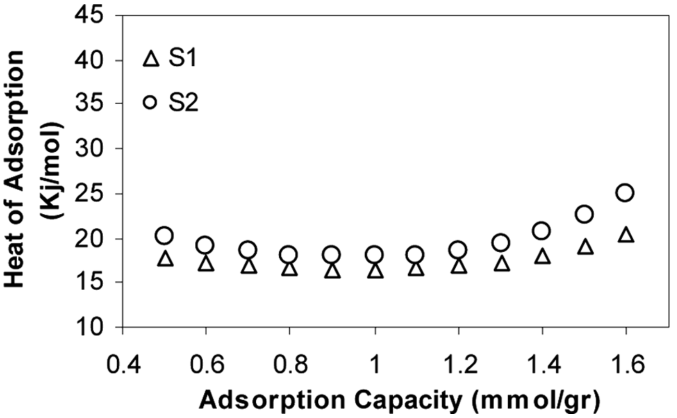

FIG. 8. Heat of adsorption versus adsorption capacity for CH_4 on S_1 and S_2.

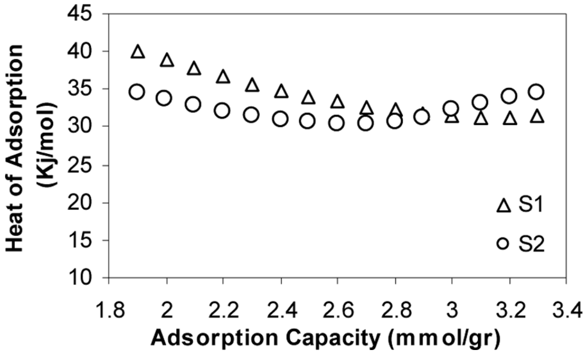

FIG 9. Heat of adsorption versus adsorption capacity for CO_2 on S_1 and S_2.

TABLE 3
Heat of adsorption ($-\Delta H_{ads}$), kJ/mol

	Adsorbent	
Adsorbate	S_1	S_2
CH_4	18.26	20.93
CO_2	33.78	32.49

using the following equation (18,25):

$$Adsorption\ selectivity = \{[mmol\ CO_2/gr\ Adsorbent]/[mmol\ CH_4/gr\ Adsorbent]\}_{T,P} \quad (4)$$

According to Figs. 10 and 11, both adsorbents show good adsorption selectivity at various temperatures. Increasing pressure above than 1000 kPa did not affect the selectivity significantly, and this result is in accordance with previous observation (31). Generally sample S_1 shows a larger adsorption selectivity especially at pressures lower than

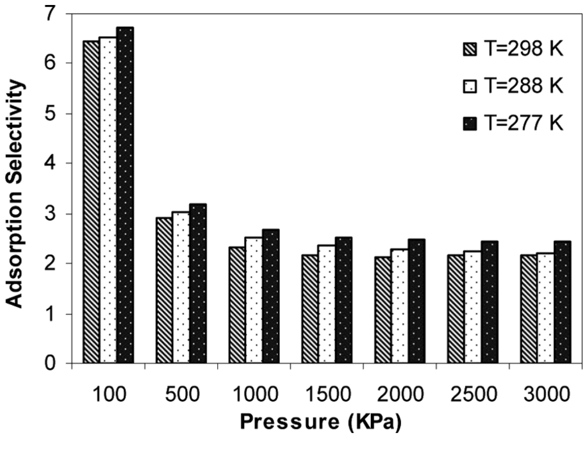

FIG. 10. Adsorption selectivity of CO_2/CH_4 on S_1 adsorbent.

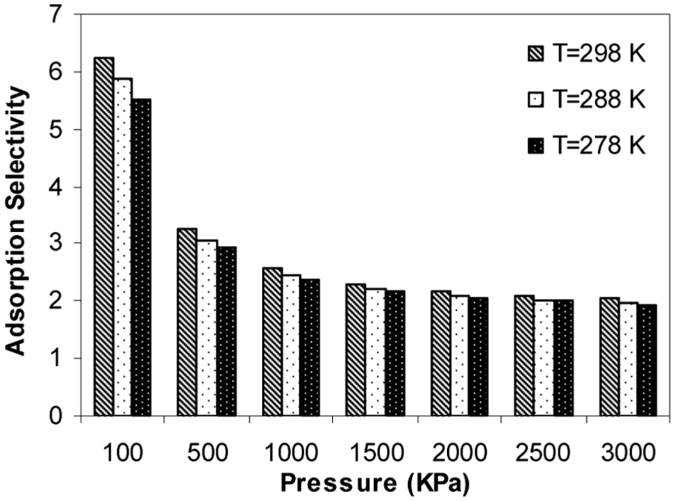

FIG. 11. Adsorption selectivity of CO_2/CH_4 on S_2 adsorbent.

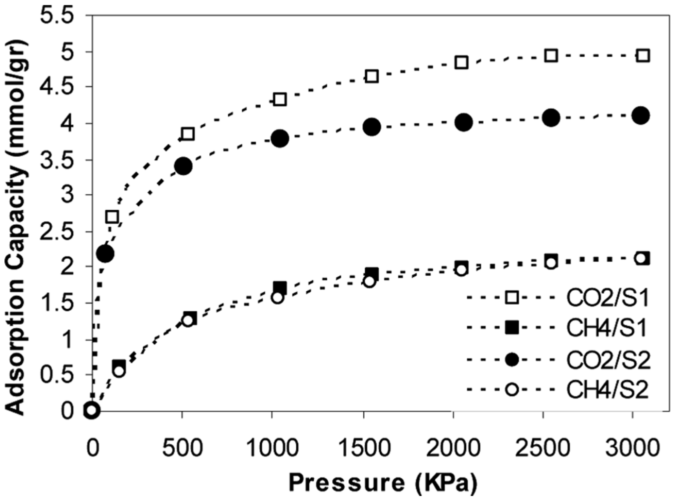

FIG. 12. Adsorption isotherm for CH_4 and CO_2 on S_1 and S_2 at 278 K.

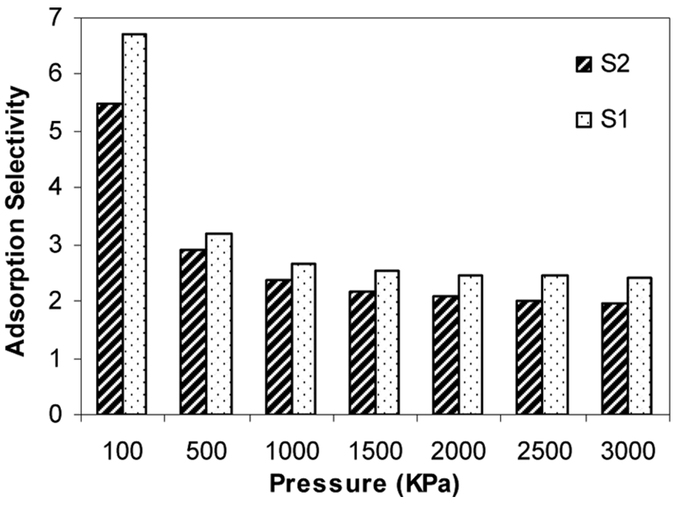

FIG. 13. Adsorption selectivity of CO_2/CH_4 on S_1 and S_2 at 278 K.

1000 kPa. However, the selectivity of CO_2/CH_4 is influenced by temperature. The adsorbate-adsorbent interaction increases by decreasing temperature due to the kinetic energy reduction of adsorbate at low temperatures, therefore CO_2, with quadrupole moment, adsorbs more strongly than the non-polar CH_4 at lower temperatures. The CO_2/CH_4 selectivity is enhanced by decreasing the temperature for sample S_1, whereas for sample S_2 it decreases by lowering the temperature. Higher heat of adsorption and affinity of S_1 towards CO_2 adsorption could be the reason of greater selectivity of S_1 at lower temperatures.

Figures 12 and 13 are the adsorption isotherms and selctivity of both gases on the two samples at 278 K. Significantly higher adsorption capacity and selectivity of sample S_1 (Si/Al = 0.2) can be observed.

CONCLUSION

In this study SAPO-34 was synthesized by sol-gel preparation method with two different Si/Al ratio (0.2 and 0.3), and the resulted products were examined for the equilibrium adsorption of carbon dioxide and methane in a wide range of pressure from normal to 3000 kPa and three levels of temperatures from 277 to 298 K.

The isotherm equations were well fitted on Toth equation and the parameters were determined. The isotherm parameters confirm the heterogenity of the SAPO-34 surface in adsorption of CO_2 and CH_4. In addition the heat of adsorption of the mentioned gases was determined using the experimental pressure-temperature equilibrium values. The equilibrium adsorption values revealed that decreasing Si/Al ratio from 0.3 to 0.2 improved the adsorption capacity and selectivity of CO_2 against CH_4.

At similar conditions to the work of Li et al. (26), 298 k and atmospheric pressure, the synthesized sample (S_1) of the present study showed a higher selectivity of CO_2/CH_4 (6.4 against 5.8, respectively).

In conclusion, synthesized SAPO-34 based on proposed procedure with (Si/Al) = 0.2 can be regarded as a good adsorbent for the enhancement of natural gas properties and purification of CH_4 from CO_2.

NOMENCLATURE

i, Dimensionless	Index of components (i = CO_2, CH_4)
p, kPa	Pressure
q_i, mmol/g	Adsorption capacity of components
q^{sat}, mmol/g	Saturation adsorption capacity
T, K	Tempetrature
θ, Dimensionless	Fractional adsorption capacity
b, kPa^{-1}	Constant of model
n, Dimensionless	Constant of model
$(-\Delta H_{ads})_i$, kJ/mol	Heat of adsorption in specific adsorption capacity
$(-\Delta H_{ads})_{av}$, kJ/mol	Average heat of adsorption

REFERENCES

1. Deglado, J.A.; Uguina, A.M.; Gomez, M.G.; Ortega, L. (2006) Adsorption equilibrium of carbon dioxide, methane and nitrogen onto Na- and H-mordenite at high pressures. *J. Separation and Purification Technology*, 48 (3): 223.
2. Baker, R.W. (2002) Future in directions of membrane gas separation technology. *Industrial Engineering Chemistry Research*, 41: 1393.
3. Martens, J.A.; Grobet, P.J.; Jacobs, P.A. (1990) Catalytic activity and Si, Al, P ordering in microporous silicoaluminophosphates of the SAPO-5, SAPO-11, and SAPO-37 type. *J. of Catalysis*, 126 (1): 299.
4. Tan, J.; Liu, Z.; Bao, X.; Liu, X.; Han, X.; He, C.; Zhai, R. (2002) Crystallization and Si incorporation mechanisms of SAPO-34. *J. Microporous and Mesoporous Materials*, 53 (1–3): 97.
5. Wendelbo, R.; Akporiaye, D.; Andersen, A.; Dahl, I.M.; Mostad, H.B. (1996) Synthesis, characterization and catalytic testing of SAPO-18, MgAPO-18, and ZnAPO-18 in the MTO reaction. *J. Applied Catalysis A: General*, 142 (2): 197.
6. Izadbakhsh, A.; Farhadi, F.; Khorasheh, F.; Sahebdelfar, S.; Asadi, M.; Yan, Z.F. (2008) Key Parameters in hydrothermal synthesis and characterization of low silicon content SAPO-34 molecular sieve. *J. Microporous and Mesoporous Materials*, article in press.
7. Jhung, S.H.; Chang, J.S.; Hwang, J.S.; Park, S.E. (2003) Selective formation of SAPO-5 and SAPO-34 molecular sieves with microwave irradiation and hydrothermal heating. *J. Microporous and Mesoporous Materials*, 64 (1–3): 33.
8. Zhao, X.S.; Lu, G.Q.; Whittaker, A.K.; Drennan, J.; Xu, H. (2002) Influence of Synthesis Parameters on the formation of mesoporous SAPOs. *J. Microporous and Mesoporous Materials*, 55 (1): 51.
9. Barrer, R.M. (1982) *Hydrothermal Chemistry of Zeolites*; Academic Press: New York, USA.
10. Szostak, R. (1989) *Molecular Sieves: Principal of Synthesis and Identification*; Van Nostrand Reinhold: New York, USA.
11. Hernández-Huesca, R.; Díaz, L.; Aguilar-Armenta, G. (1999) Adsorption equilibria and kinetics of CO_2, CH_4 and N_2 in natural zeolites. *J. Separation and Purification Technology*, 15 (2): 163.
12. Armaroli, T.; Simon, L.J.; Digne, M.; Montanari, T.; Bevilacqua, M.; Valtchev, V.; Patarin, J.; Busca, G. (2006). Effects of crystal size and Si/Al ratio on the surface properties of H-ZSM-5 zeolites. *J. Applied Catalysis A: General*, 306: 78.
13. Mintova, S.; Valtchev, V.; Onfroy, T.; Marichal, C.; Knözinger, H., Bein, T. (2006). Variation of the Si/Al ratio in nanosized zeolite Beta crystals. *J. Microporous and Mesoporous Materials*, 90 (1–3): 237.
14. Tan, J.; Liu, Z.; Bao, X.; Liu, X.; Han, X.; He, C.; Zhai, R. (2002) Crystallization and Si incorporation mechanisms of SAPO-34. *J. Microporous and Mesoporous Materials*, 53 (1–3): 97.
15. Huesca, R.H.; Diaz, L.; Armenta, G.A. (1999) Adsorption equilibria and kinetics of CO_2, CH_4 and N_2 in natural zeolites. *J. Separation and Purifcation Technology*, 15 (2): 163.
16. Himeno, S.; Tomita, T.; Suzuki, K.; Yoshida, S. (2007) Characterization and selectivity for methane and carbon dioxide adsorption on the all-silica DD3R zeolite. *J. Microporous and Mesoporous Materials*, 98 (1–3): 62.
17. Mirfendereski, S.M.; Mazaheri, T.; Sadrzadeh, M.; Mohammadi, T. (2008) CO_2 and CH_4 permeation through T-type zeolite membranes: Effect of synthesis parameters and feed pressure. *J. Separation and Purification Technology*, 61 (3): 317.
18. Hong, M.; Li, S.; Funke, H.F.; Falconer, J.L.; Noble, R.D. (2007) Ion-exchanged SAPO-34 membranes for light gas separations. *J. Microporous and Mesoporous Materials*, 106 (1–3): 140.
19. Harlick, P.J.E.; Tezel, F.H. (2003) Adsorption of carbon dioxide, methane and nitrogen: Pure and binary mixture adsorption for ZSM-5 with SiO_2/Al_2O_3 ratio of 280. *J. Separation and Purification Technology*, 33 (2): 199.
20. Liu, X.; Zhao, L.; Fu, X.; Sun, Y.; Su, W.; Zhou, Y. (2007) Adsorption and regeneration study of the mesoporous adsorbent SBA-15 adapted to the capture/separation of CO_2 and CH_4. *J. Chemical Engineering Science*, 62 (4): 1101.
21. Perez, E.G.; Ania, J.B.; Parra, J.B.; Sanchez, A.G.; Van Baten, J.M.; Krishna, R.; Dubbeldam, D.; Calero, S. (2007) A computational study of CO_2, N_2, and CH_4 adsorption in zeolites. *J. Adsorption*, 13 (5–6): 469.
22. Delgado, J.A.; Uguina, M.A.; Sotelo, J.L.; Ruiz, B.; Gomez, J.M. (2006) Fixed- bed adsorption of carbon dioxide/methane mixtures on silicalite pellets. *J. Adsorption*, 12 (1): 5.
23. Walton, K.S.; Abney, M.B.; LeVan, M.D. (2006) CO_2 adsorption in Y and X zeolites modified by alkali metal cation exchange. *J. Microporous and Mesoporous Materials*, 91 (1–3): 78.
24. Cui, Y.; Kita, H.; Okamoto, K. (2004) Preparation and gas separation performance of zeolite T membrane. *J. Material Chemistry*, 14 (1–2): 924.
25. Li, S.; Falconer, J.L.; Noble, R.D. (2008) SAPO-34 membranes for CO2/CH4 separation: Effect of Si/Al ratio. *J. Microporous and Mesoporous Materials*, 110 (1–3): 310.
26. Li, S.; Falconer, J.L.; Noble, R.D. (2004). SAPO-34 membranes for CO2/CH4 separation. *J. Membrane Science*, 241 (1): 121.
27. Mertens, M.; Strohmaier, K.G. Process for manufacture of molecular sieves. U.S. Patent 7,052,664 B2, May 30, 2006.
28. Gholamhosseiny, M.; Fatemi, S.; Rasoolzadeh, M. (2008) Hydrogen adsorption and equilibrium models on multi-walled carbon nanotubes at moderate temperatures and pressures. *International Journal of Chemical Reactor Engineering*, 6: A80.
29. Prakash, A.M.; Unnikrishnan, S. (1994). Synthesis of SAPO-34: High silicon incorporation in the presence of morpholine as template. *J. of the Chemical Society*, Faraday Transactions, 90: 2291.
30. Do, D.D. (1998). *Adsorption Analysis: Equilibria and Kinetics*; First Edition, Imperial College Press: London, U.K.
31. Ashraf, S.S.; Fatemi, S.; Hashemi, S.J.; Omrani, P. (2008). Synthesis the fine particles of SAPO molecular sieve for effective separation of carbon dioxide from methane. 18th International Congress of Chemical and Process Engineering, (CHISA) Symposium Micro and Mesoporous materials, Aug. 23–27, Praha, Czech Republic.